2005

Rational Fraction Approximations for Passive Network Functions

William Joel Dietmar Johnson
University of South Florida

Rational Fraction Approximations for Passive Network Functions

by

William Joel Dietmar Johnson

A dissertation submitted in partial fulfillment
of the requirements for the degree of
Doctor of Philosophy
Department of Electrical Engineering
College of Engineering
University of South Florida

Major Professor: Arthur David Snider, Ph.D.
Mourad Ismail, Ph.D.
Evguenii A. Rakhmanov, Ph.D.
Stanley Kranc, Ph.D.
Kenneth A. Buckle, Ph.D.

Date of Approval:
March 21, 2005

Keywords: approximation theory, passive filters, Padé-Chebyshev approximation

Dedication

To my wife, Sandy.

Acknowledgments

I wish to acknowledge my main advisor, Dr. Arthur David Snider, for his constant help, guidance, and encouragement.

Table of Contents

List of Tables

List of Figures

Rational Fraction Approximations for Passive Network Functions

William Joel Dietmar Johnson

ABSTRACT

In electrical engineering, the designer is often presented with the problem of synthesizing a circuit for which the mathematical specifications are unsuitable for physical realization. Hence, the engineer must approximate as well as possible the prescribed network function by another function which is realizable. This paper describes a new approximation method for solving the problem of realizing passive network transfer functions, where the realization is carried out through the use of passive, reciprocal, lumped, linear, and time-invariant elements.

Chapter 1

Introduction

1.1 Motivation

Network synthesis is the study of obtaining a prescribed input to output mathematical relationship utilizing physically realizable elements. This dissertation will present a new approximation method for obtaining a physically realizable transfer function from the stated requirements. The method is a novel synthesis of known techniques from analytic approximation theory and filter design. We will concern ourselves with those networks that are passive, lumped, linear, reciprocal, and time-invariant. The network shall be realized as a device with a single input port and a single output port, or two-port.

Transfer functions realized by passive networks are always stable, i.e., for a bounded input these circuits produce a bounded output. Stability translates into a requirement on the network function: it must be analytic in the open right half of the complex plane, and if poles are on the imaginary axis they must be first order. Depending on the desired network realization, there may be additional requirements on the residues of the transfer function [17]. Physical networks, such as we describe, require an additional condition: the transfer function must be a rational function, numerator degree $\leq$ denominator degree, with real coefficients.

Network synthesis is subdivided into the approximation problem and the realization problem. The realization problem, the process of obtaining the physical network

element values and their connected graph, is not the focus of this dissertation and will not be further discussed.

1.2 Background

The rules of engagement for circuit theory are detailed in references [1] and [10]. In what follows we will present only those facts pertinent to this body of work.

Instead of working with the integro-differential circuit equations in the "time domain", engineers frequently make use of the Laplace transform

$$F(s) = \int_{0^-}^{\infty} f(t)e^{-st}dt$$

and work in the "frequency domain". The Laplace variable, s, is interpreted as complex frequency, $s = \sigma + j\omega$, where σ is attenuation and ω is frequency ($j = \sqrt{-1}$, see Appendix A). This transform allows the engineer to use algebra for most computations.

The three basic circuit components for physical realization are the resistor, capacitor, and inductor. The algebraic relationship between voltage and current in each of these components is Ohm's Law

$$V(s) = Z(s)I(s)$$

where $V(s)$ is the Laplace transformed voltage, $I(s)$ is the Laplace transformed current, and $Z(s)$ is the impedance. Figure 1 shows these basic elements and their values for $Z(s)$.

When R, C, and L elements are connected into a network and only two points of access are allowed, such as in Figure 2, the configuration can be interpreted as a two-port network. A port is a point at which access to a network may be gained.

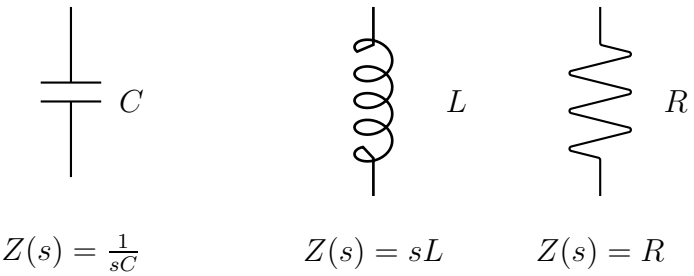

Figure 1. Network Elements.

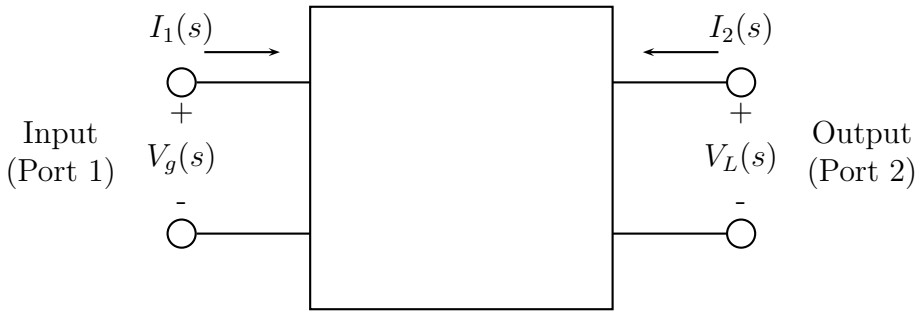

Figure 2. Two-port Network.

The importance of the two-port concept is that individual element behavior can be replaced by larger-scale collective behavior by describing the output as a transformed version of the input. There are only four methods for describing these transformations. They are

$$\frac{V_L(s)}{V_g(s)}, \text{dimensionless voltage transfer function,}$$

$$\frac{V_L(s)}{I_1(s)}, \text{transfer impedance function,}$$

$$\frac{I_2(s)}{I_1(s)}, \text{dimensionless current transfer function,} \tag{1}$$

and

$$\frac{I_2(s)}{V_g(s)}, \text{transfer admittance function.}$$

The laws of circuit theory dictate that each of these transfer functions is a real rational function of s.

It is a matter of choice to the engineer which network transfer function is to be utilized. The symbol we shall use in this body of work to describe a generic network transfer function is $G(s)$.

A network may be realized with either two of the types of circuit component elements (RC, RL, or LC) or all three elements (RLC). The location of the poles and zeros of the network transfer function may have additional constraints. Table 1 summarizes these constraints.

1.3 Classical Filter Magnitude Design Method

A filter is a two-port network which selectively passes some frequencies with little attenuation, while greatly attenuating all other frequencies. Classical filter design techniques focus on finding realizable rational transfer functions $G_{ratl}(s)$ whose magnitudes approximate, for $s = j\omega$, one of the 4 ideal filter specifications, $H_{spec}(\omega)$, shown in Figure 3.

In fact, using well-known rational-function transformations of the frequency variable, one can translate the latter three (band-pass, high-pass, band-stop) specifications to the first (prototype). This results in a simplification known as the low-pass prototype (LPP). The LPP dependent variable, $\tilde{s} = \tilde{\sigma} + j\tilde{\omega}$, plays the same role as the original Laplace variable s. The requirements imposed on the LPP are transformed from $H_{spec}(\omega)$ to become $\tilde{H}_{spec}(\tilde{\omega})$.

The class of rational approximants traditionally used is restricted to simple reciprocals of polynomials; these have the appropriate numerator-denominator degree

Table 1. Placement of Poles and Zeros for Various Network Functions. [8]

Locations of Poles and Zeros				
	LC[a]		RC or RL[a]	
Function	**Poles**	**Zeros**	**Poles**	**Zeros**
Transfer functions of ladder networks[b]	Simple on $j\omega$ axis[c]	Any order on $j\omega$ axis[d]	Simple on negative real axis[c]	Any order on negative real axis[d]
General transfer functions[e]	Simple on $j\omega$ axis[c]	Any order on $j\omega$ axis[d]; quadrantal symmetry in right- and left-half planes	Simple on negative real axis[c]	Any order in right- or left-half plane[d,f]
	RLC[a]			
Function	**Poles**		**Zeros**	
Transfer functions of ladder networks	Any order in left-half planes[c,g]		Any order in left-half plane or on $j\omega$ axis[d]	
General transfer functions	Any order in left-half plane[c,g]		Any order in right- or left-half plane[d,f]	

[a]Excluding mutual inductance.

[b]Ladder networks are connections of components where only adjacent neighbors in one plane are allowed.

[c]Transfer immittances may have poles at the origin and infinity but dimensionless transfer functions may not.

[d]Including the origin and infinity.

[e]General networks are connections of components where non-adjacent neighbors in multiple planes are allowed.

[f]The positive real axis is excluded unless balanced networks are permitted.

[g]Any poles on the $j\omega$ axis must be simple.

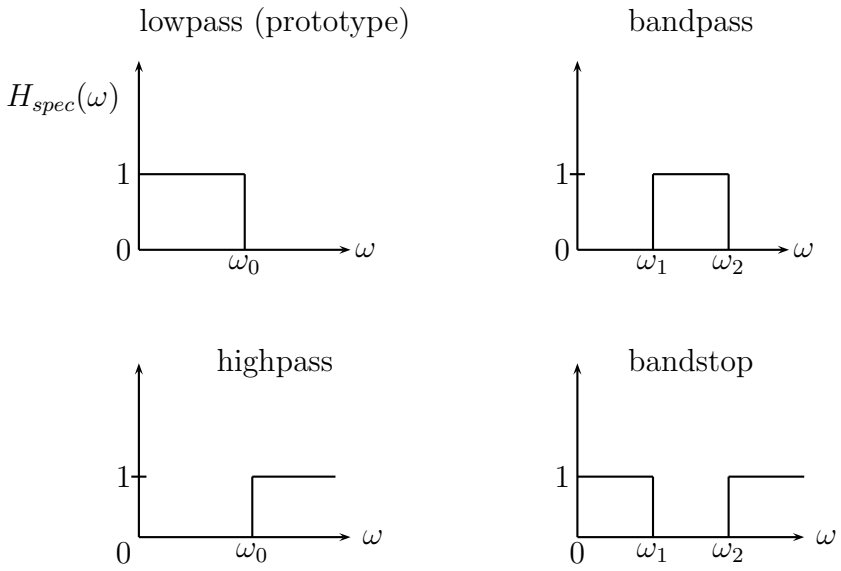

Figure 3. Filter Types.

relation, so the polynomial is constructed to approximate the reciprocal of the filter, on the filter's support. Butterworth filters, for example, take the form: for $\tilde{\omega}$ real, $\tilde{H}_{spec}(\tilde{\omega}) \simeq |\tilde{G}_{ratl}(j\tilde{\omega})|$, let

$$\tilde{G}_{ratl}(j\tilde{\omega}) = \frac{1}{1 + A(\tilde{\omega})} \tag{2}$$

with polynomial $A(\tilde{\omega})$, $A(0) = 0$, $A(1) = 1$, $A(\tilde{\omega})$ "maximally flat" at 0, Figure 4.

This dissertation addresses the possibility of devising rational transfer functions that approximate more exotic design specifications, such as indicated in Figures 5 and 6. We acquire additional flexibility by utilizing the *full* class of rational functions with the appropriate asymptotic behavior (denominator degree exceeding numerator degree for design specifications with bounded support). The Padé-Chebyshev methodology is used to construct the approximant in the interval containing the support (supplemented with some adjustments ensuring the physical realizability of the transfer function).

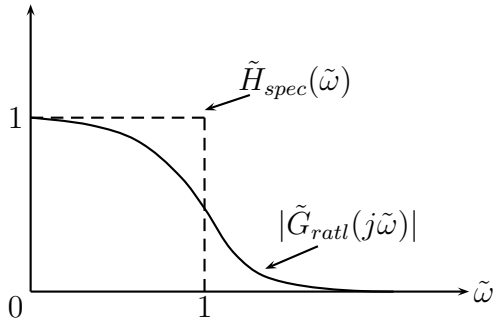

Figure 4. Butterworth Filter.

1.4 Non-traditional Filters

In equation (2) of Section 1.3, we see that the traditional $\tilde{G}_{ratl}(j\tilde{\omega})$ is not the most general rational function. As a result, the restricted form has difficulties approximating more exotic filters such as in Figure 5 or in Figure 6. Figure 5 is an example of a double bandpass filter and Figure 6 is an example of a ramp lowpass filter. The classical approximation method is unsuited for filter realizations such as these. A more sophisticated method, exploiting more general rational functions, is needed.

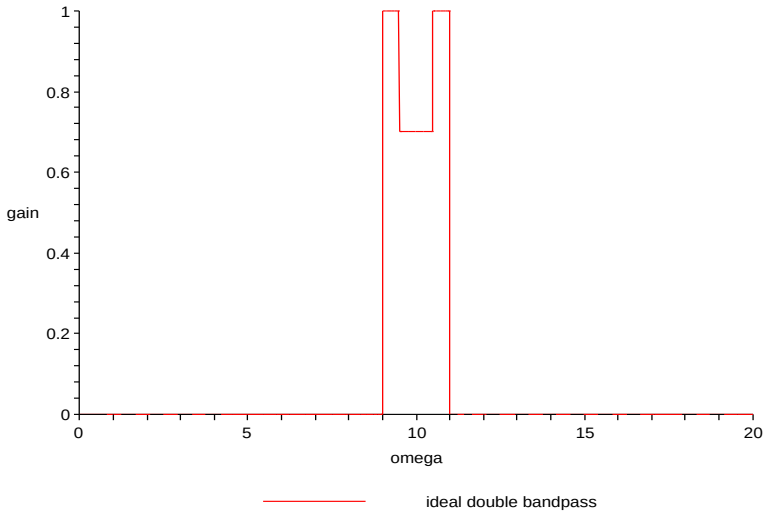

Figure 5. Double Bandpass Filter Frequency Response.

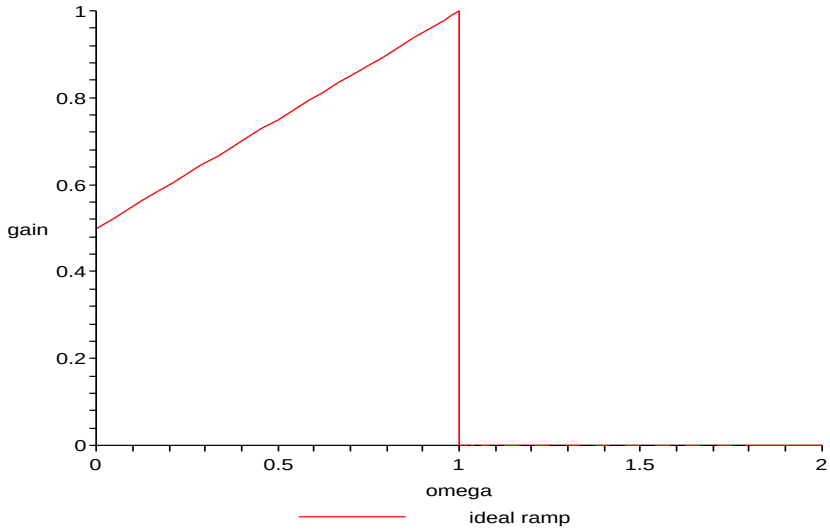

Figure 6. Ramp Lowpass Frequency Response.

1.5 Watanabe's Double Bandpass Filter Design

In 1961, H. Watanabe wrote a filter theory paper introducing his solution to the double bandpass filter problem [16], similar to the filter shown in Figure 5. The methodology is quite complex, and is summarized in Appendix B. Ultimately, the following transfer function is derived:

$$G(s) = \frac{s^2(s^2+.717095)}{(s^2+.162918s+.128222)(s^2+.072328s+.275307)} \times \frac{(s^2+.332031)}{(s^2+.693687s+2.103897)(s^2+.152983s+.984953)}, \quad (3)$$

which has a frequency response (shown with a log-log axis to scale its features) given in Figure 7.

It is the contribution of this dissertation to put forth a new method for obtaining a double bandpass filter, which is substantially simpler than Watanabe's in both concept and implementation. Moreover, this new method allows for more general shapes than just double bandpass filters (e.g. Figure 6).

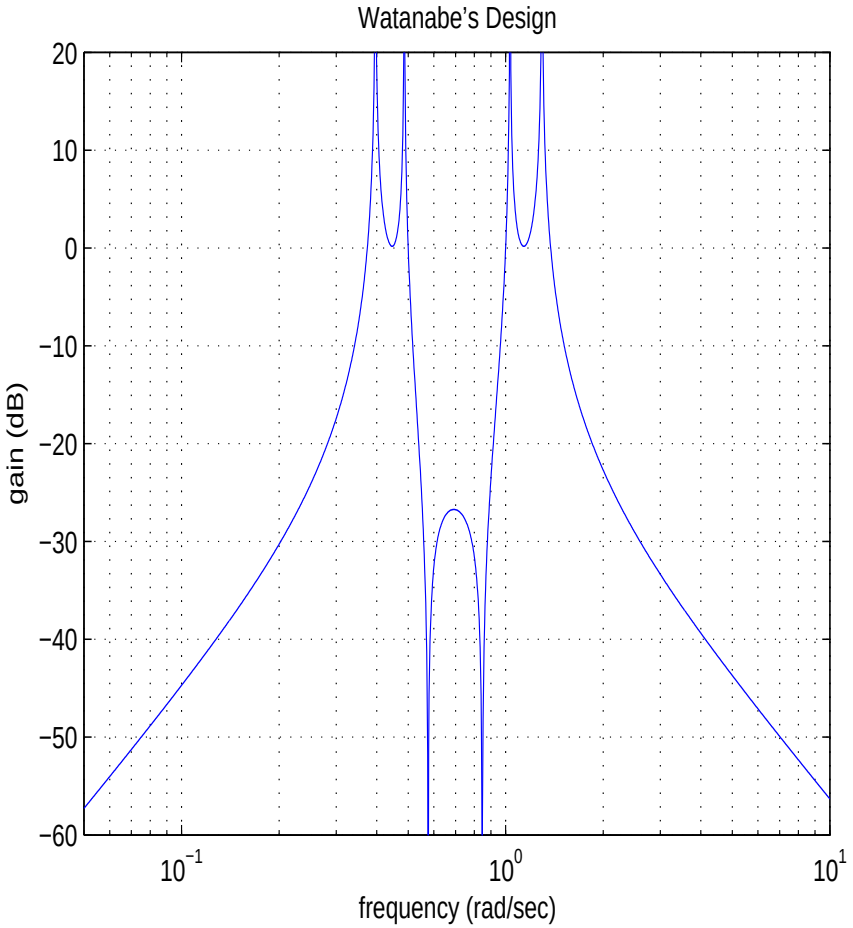

Figure 7. Watanabe's Design Example: Bandpass Nontraditional Frequency Response.

Chapter 2

Algorithm

By combining polynomial approximation theory with Padé approximation methods, one can attack design specifications such as given by Figures 5 and 6, or more general shapes. Unfortunately, Padé methods have a major drawback—the resulting transfer function may be unstable. In this chapter, we will describe a novel design procedure, using the extra flexibility of the Padé - Chebyshev method together with the technique of Spectral Factorization [4], to design physically realizable network transfer functions for some of the specifications which have been confounded by classical methods. The algorithm allows the designer to choose m, numerator degree, and n, denominator degree, such that the magnitude of $G_{ratl}(s)$, for $s = j\omega$, approximates the desired specification in $\omega \in [0, 1]$ and achieves the desired attenuation in $\omega \in [1, \infty)$.

2.1 Strategy

An outline of our proposed strategy for obtaining $G_{ratl}(s)$ from a given finitely supported nonnegative $H_{spec}(\omega)$, $0 \leq \omega < \infty$, is to

1. Devise a convenient analytic mapping $\tilde{\omega} = f(\omega)$ such that the support of $H_{spec}(\omega)$ is mapped inside $[-1, 1]$ and the transformed specification, $\tilde{H}_{even}(\tilde{\omega})$, is an even function in $(-\infty, \infty)$. Further conditions on this mapping will be elaborated below.

2. Mollify $\tilde{H}_{even}(\tilde{\omega})$ on its support to obtain a continuous and bounded variate function, $\tilde{H}_{cont}(\tilde{\omega})$.

3. Compute a Padé-Chebyshev rational approximation to $max\{\frac{1}{|\tilde{H}_{cont}(\tilde{\omega})|^2}, A\}$ for some large A on $\omega \in [-1, 1]$ using Geddes' algorithm; take $m > n$ in order to satisfy the desired attenuation. Denote this result as $r_{m,n}(\tilde{\omega})$.

4. For $\tilde{s} = j\tilde{\omega}$, define $R_{m,n}(\tilde{s}) = \frac{1}{r_{m,n}(\tilde{s}/j)}$ and analytically continue $R_{m,n}(\tilde{s})$ to the whole plane.

5. Spectrally factor the Padé-Chebyshev function, $R_{m,n}(\tilde{s})$ to obtain $\tilde{G}_{ratl}(\tilde{s})$.

6. Return to the original domain by mapping $\tilde{G}_{ratl}(\tilde{s})$ to $G_{ratl}(s)$. End with $G_{ratl}(s)$, which

    a. is rational, physically realizable

    b. $|G_{ratl}(j\omega)| \simeq H_{spec}(\omega)$ on support of $H_{spec}(\omega)$, due to Padé-Chebyshev construction.

    c. $|G_{ratl}(j\omega)| \to 0$ as $\omega \to \infty$ because denominator degree $>$ numerator degree.

7. Iterate as necessary. By either modifying $H_{cont}(\omega)$, m, n, A, or mapping, try to bring $|G_{ratl}(j\omega)|$ into closer agreement with $H_{spec}(\omega)$.

In our examples, we will utilize standard rational mappings from classical design methods for step 2, see Appendix C.

2.2 Flowchart

The following is a flowchart of our algorithm. Note: the function $\tilde{H}_{cont}(\tilde{\omega})$ is squared so that we may spectral factor in a later step.

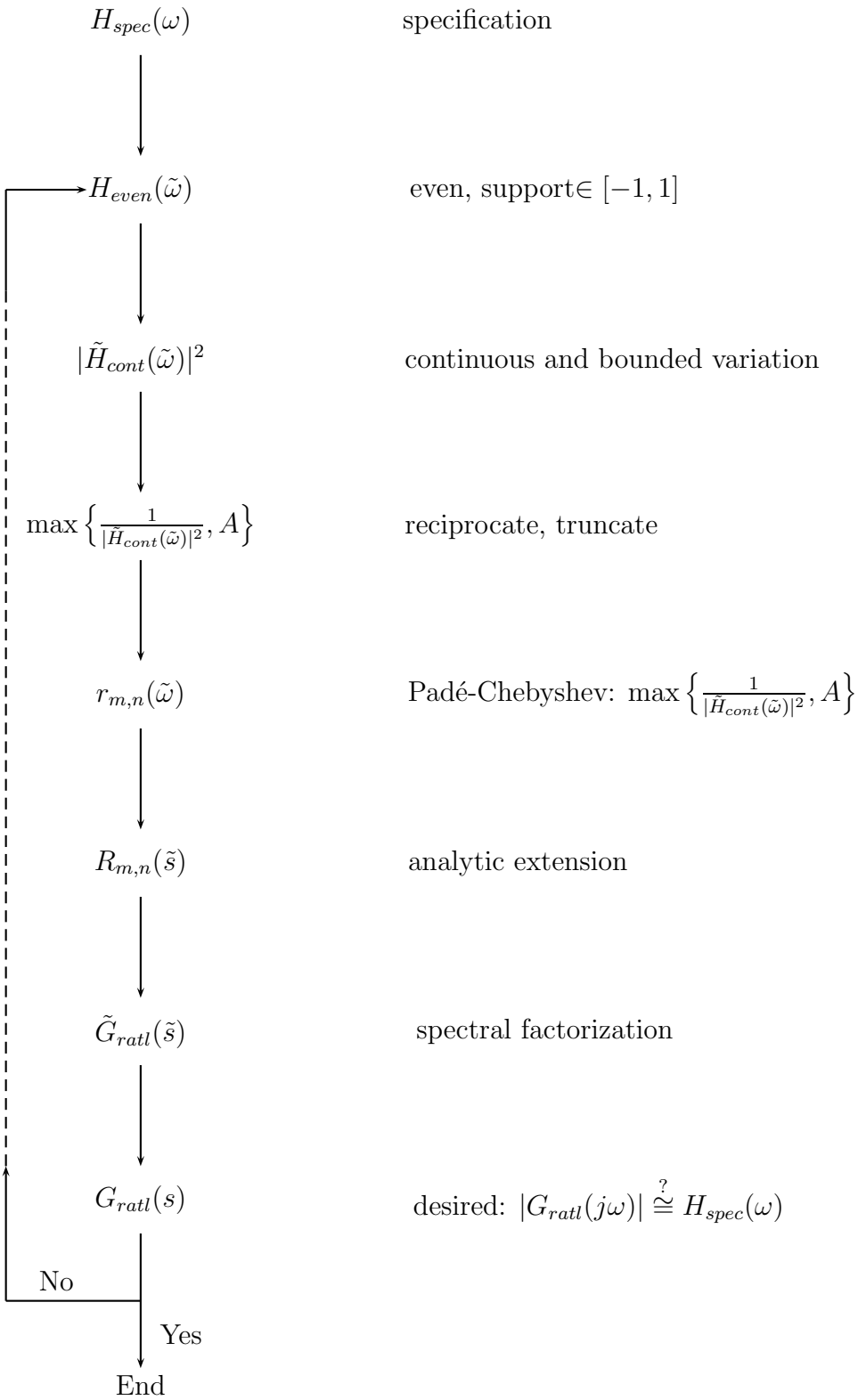
$H_{spec}(\omega)$
specification
$H_{even}(\tilde{\omega})$
even, support$\in [-1,1]$
$|\tilde{H}_{cont}(\tilde{\omega})|^2$
continuous and bounded variation
$\max\left\{\frac{1}{|\tilde{H}_{cont}(\tilde{\omega})|^2}, A\right\}$
reciprocate, truncate
$r_{m,n}(\tilde{\omega})$
Padé-Chebyshev: $\max\left\{\frac{1}{|\tilde{H}_{cont}(\tilde{\omega})|^2}, A\right\}$
$R_{m,n}(\tilde{s})$
analytic extension
$\tilde{G}_{ratl}(\tilde{s})$
spectral factorization
$G_{ratl}(s)$
desired: $|G_{ratl}(j\omega)| \stackrel{?}{\cong} H_{spec}(\omega)$
No
Yes
End

2.3 Padé Approximation

Polynomial approximation is the dominant method for obtaining physically realizable transfer functions for classical filters. Polynomial methods have some distinct advantages:

1. For any continuous function on a given closed interval $[a, b]$ and for any $\epsilon > 0$, there always exists an algebraic polynomial of sufficient degree that can approximate the original function to within any given tolerance ϵ [2].

2. The coefficients in the polynomial can often be obtained by a linear system of equations.

But there are some distinct disadvantages:

1. A high polynomial degree is generally needed for accuracy.

2. The restricted form of $\tilde{G}_{ratl}(j\tilde{\omega})$ in Equation (2) cannot approximate zeroes within the support of $\tilde{H}_{cont}(\tilde{\omega})$.

A method that may overcome these deficiencies is rational approximation. Because every polynomial is a rational function, approximation using rational functions yields results that are no worse than polynomial approximation. An advantage of rational functions is that functions with the numerator and denominator having the same or nearly the same degree will generally produce approximation results superior to those with polynomials, for the same amount of computational effort [2]. In general, the methods for obtaining the unknown coefficients are not linear. One computational method whereby the unknown coefficients of the rational function are obtained through a linear system of equations is due to H. Padé [14]. The Padé approximation technique is an extension of the Taylor polynomial approximation method.

We reserve the variables ω, $\tilde{\omega}$, and H for our design problem and use the variable x and f for the present exposition. The Padé approach is as follows. If $h(x)$ is analytic and

$$h^{(k)}(0) = 0 \ \text{ for each } \ k = 0, 1, \cdots, N, \ \text{ then} \tag{4}$$

$$h \ \text{ has a zero of multiplicity } \ (N+1) \text{ at } \ x = 0 \ [3].$$

Suppose an arbitrary function f satisfies

$$f(x) \simeq \sum_{i=0}^{N} a_i x^i + O(x^{N+1}), \tag{5}$$

then $r_{m,n}$ is a Padé approximation of order (m, n) to f, if

$$r_{m,n}(x) = \frac{p(x)}{q(x)} = \frac{p_0 + p_1 x + p_2 x^2 + \cdots + p_m x^m}{1 + q_1 x + q_2 x^2 + \cdots + q_n x^n} = \frac{\sum p_i x^i}{\sum q_i x^i} \ \text{ with } q_0 \equiv 1 \tag{6}$$

and

$$f^{(k)}(0) - r^{(k)}(0) = 0, \ \text{ for } k = 0, 1, 2, \ldots, N, \tag{7}$$

where $N = m+n$. Note that there are $N+1$ free parameters $(p_0,\ p_1, \cdots, p_m,\ q_1,\ q_2, \cdots, q_n)$ available for enforcing (7).

Using (6), we have

$$\begin{aligned} f(x) - r_{m,n}(x) &= f(x) - \frac{p(x)}{q(x)} \\ &= \frac{f(x)q(x) - p(x)}{q(x)} \\ &= \frac{\sum_{i=0}^{N} a_i x^i \sum_{i=0}^{n} q_i x^i - \sum_{i=0}^{m} p_i x^i}{\sum_{i=0}^{m} q_i x^i} + O(x^{N+1}). \end{aligned} \tag{8}$$

From equation (4), with $h = f - r$, we require the numerator of equation (8) to have no terms of degree $\leq N$, i.e., the coefficients of $x^k = 0$ for $k = 0, 1, \cdots, N$. Or,

$$(a_0 + a_1 x + \cdots + a_N x^N)(1 + q_1 x + \cdots + q_n x^n) - (p_0 + p_1 x + \cdots + p_m x^m) = O(x^{N+1}).$$

Expanding and collecting terms for each x^k yields [5],

$$\left[\left(\sum_{i=0}^{k} a_i q_{k-i}\right) - p_k\right] x^k = 0, \quad k = 0, 1, \cdots, N \tag{9}$$

(where we take p_i or q_i to be zero when the subscript is out of range).

Display (9) is a set of $N + 1$ linear equations. Note that if the coefficients $\{a_i\}$ in the Taylor approximation (5) to f are real, then the coefficients $\{p_i, q_i\}$ in the Padé approximation will also be real.

Example: For $n = m = 2$, find the Padé approximation for $f(x) = e^x$. The Taylor series expansion for e^x is

$$e^x = \sum_{i=0}^{\infty} \frac{x^i}{i!}.$$

The first 5 terms are

$$e^x \approx 1 + x + \frac{x^2}{2} + \frac{x^3}{6} + \frac{x^4}{24}.$$

Enforcing equation (9) with $n = m = 2$;

$$\begin{aligned}
x^4 &: \quad \frac{1}{2}q_2 + \frac{1}{6}q_1 + \frac{1}{24} = 0 \\
x^3 &: \quad q_2 + \frac{1}{2}q_1 + \frac{1}{6} = 0 \\
x^2 &: \quad q_2 + q_1 + \frac{1}{2} = p_2 \\
x^1 &: \quad q_1 + 1 = p_1 \\
x^0 &: \quad 1 = p_0.
\end{aligned}$$

Solving the above system yields

$$q_0 \equiv 1,\ q_1 = -\frac{1}{2},\ q_2 = \frac{1}{12}$$

$$p_0 = 1,\ p_1 = \frac{1}{2},\ p_2 = \frac{1}{12}$$

$$r_{2,2}(x) = \frac{\frac{1}{12}x^2 + \frac{1}{2}x + 1}{\frac{1}{12}x^2 - \frac{1}{2}x + 1} = \frac{x^2 + 6x + 12}{x^2 - 6x + 12}.$$

A plot of the error, $r_{2,2}(x) - e^x$, is shown in figure 8.

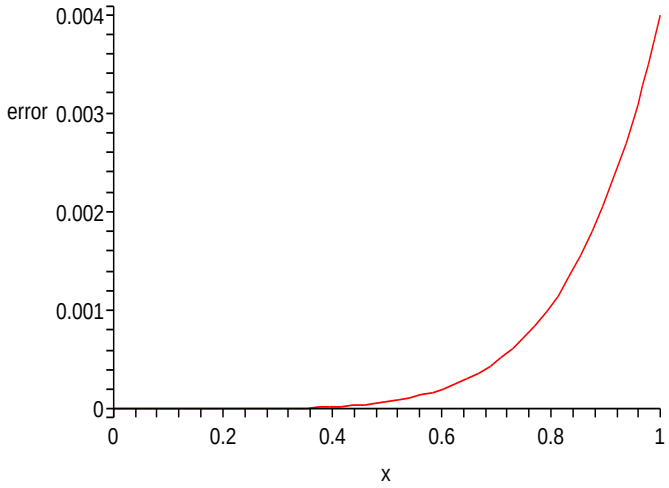

Figure 8. Error of e^x vs. $r_{2,2}(x)$ Frequency Response.

2.4 Padé-Chebyshev Approximation

A problem with the regular Padé method is that it can yield poor approximations over an *interval*, because the regular Padé method requires matching derivatives at only one point. In an attempt to decrease the approximation error over an interval,

one can expand the given $f(x)$ using Chebyshev polynomials of the first kind,

$$f(x) = \sum_{k=0}^{\infty\,\prime} c_k T_k(x), \tag{10}$$

$$\text{where} \quad T_k(x) = \cos(k \cos^{-1} x)$$

$$\text{and} \quad \sum_{k=0}^{\infty\,\prime} u_k = \frac{1}{2}u_0 + u_1 + u_2 + \ldots$$

$$\text{and} \quad c_k = \frac{2}{\pi}\int_{-1}^{1} \frac{f(x)T_k(x)}{\sqrt{1-x^2}}dx, \tag{11}$$

and truncate this expansion. If $f(x) \in C[-1,1]$ and has bounded variation on the interval $[-1,1]$, then $\sum_{k=0}^{\infty\prime} c_k T_k(x)$ converges uniformly to $f(x)$ [12].

The Padé-Chebyshev approximant to $f(x)$ is defined as that rational function,

$$r_{m,n}(x) = \frac{\sum_{k=0}^{m} p_k x^k}{\sum_{k=0}^{n} q_k x^k}, \tag{12}$$

such that for some integer N,

$$f(x) - r_{m,n}(x) = \sum_{k=N+1}^{\infty} d_k T_k(x).$$

The algorithm due to Geddes [6], is

1. With assumptions on $f(x)$, stated above, choose an integer N and form $\tilde{f}_N(x)$ by truncating the Chebyshev series for $f(x)$ after $N+1$ terms

$$\tilde{f}_N(x) \simeq \sum_{k=0}^{N\,\prime} c_k T_k(x), \tag{13}$$

with c_k as in (11).

2. Carry the values of $\tilde{f}_N(x)$ from the interval $[-1, 1]$ in the $x-$domain to the unit circle $C = \{z : |z| = 1\}$ in the $z-$domain using the two-to-one mapping

$$z = x \pm j\sqrt{1 - x^2}$$

to obtain

$$\hat{f}_N(z) \simeq \sum_{k=0}^{N}{}' c_k z^k \tag{14}$$

where the polynomial coefficients in equation (14) are precisely the same as the coefficients in equation (13).

3. The polynomial in equation (14) is then approximated by the regular Padé method to yield $r_{m,n}(z)$ as previously discussed in Section 2.2. For reasons to be discussed below, in our application we take $m \geq n$.

4. Transform the regular Padé function using the mapping

$$R_{m,n}(x) = \frac{r_{m,n}(x + j\sqrt{1 - x^2}) + r_{m,n}(x - j\sqrt{1 - x^2})}{2}$$

to yield the desired Padé-Chebyshev approximation, $R_{m,n}(x)$. The explanation why this calculation yields a real, rational function with the stated degrees is given in Geddes [6]. Note further that if $f(x)$ is even, then $R_{m,n}(x)$ will also be even.

The above algorithm states a method for computing the Padé-Chebyshev approximation for $f(x)$ if the following three conditions hold [6].

1. $m > n$. This ensures that the numerator degree in the final Padé-Chebyshev approximation is, in fact, m.

2. The Padé approximant $r_{m,n}(z)$ satisfying

$$\tilde{f}_N(z) - r_{m,n}(z) = O(z^{m+n+1})$$

can be found (i.e., it is "normal").

3. The Padé approximant $r_{m,n}(z)$ has no poles lying in the closed unit disk. This ensures that $r_{m,n}(z)$ is unique.

Because the truncated Chebyshev series is a near-minimax polynomial approximation [13], it is reasonable to expect that the Padé-Chebyshev rational approximation will also be near-minimax [9].

2.5 Spectral Factorization

If a rational function, $F(s)$, with real coefficients has the property $F(s) = F(-s)$ and $F(0) > 0$, then there exists a factorization

$$F_{m,n}(s) = \hat{G}(s)\hat{G}(-s)$$

such that $\hat{G}(s)$ has all its poles and zeros in the closed left-half of the complex plane and $\hat{G}(-s)$ has its poles and zeros in the closed right-half complex plane [5]. This factorization is known as spectral factorization.

This follows because the poles and zeros of a typically real, even $F_{m,n}(s)$ occur in quadrantal symmetry with respect to both the real axis and the imaginary axis; e.g., see Figure 9. That is, the complex roots not on the imaginary axis occur in groups of four, roots on the imaginary axis occur in pairs, and roots on the real axis occur two at a time.

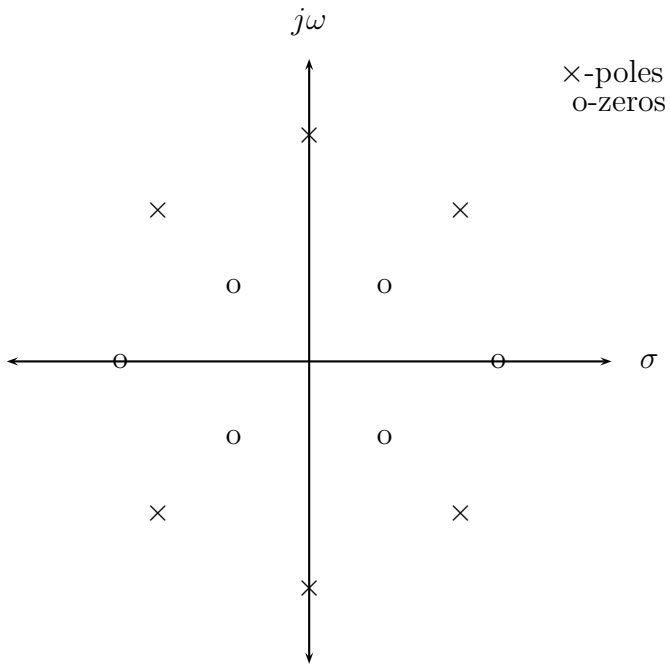

Figure 9. Poles and Zeros of an Even Real Rational Function.

The zeros and poles can be computed using a root finding algorithm on the numerator and denominator of $F_{m,n}(s)$. The desired rational factor $\hat{G}(s)$ is obtained by selecting all of the left-half-plane zeros and poles, and by selecting one-half of the imaginary axis zeros and poles [7]. Let

$$F_{m,n}(s) = l\frac{\prod(s-z_i)(s+z_i)}{\prod(s-p_i)(s+p_i)}$$

$$\text{with } Re(z_i), Re(p_i) \leq 0,$$

$$\text{then the spectral factor of } F_{m,n}(s) \text{ is } \hat{G}(s) = k\frac{\prod(s-z_i)}{\prod(s-p_i)}$$

2.6 Algorithm

As outlined in section 2.1, our algorithm has seven parts. The steps are elaborated below.

1. *Devise a mapping of the frequency axis to recast the specification* $H_{cont}(\omega)$, $\omega \in [0, \infty)$, *as an even function* $\tilde{H}_{even}(\tilde{\omega})$, $\tilde{\omega} \in (-\infty, \infty)$, *with support on* $[-1, 1]$. The mapping must be analytically extendable to the whole complex plane; it must be explicitly invertible, and when composed with rational functions, the result must yield a rational function. Furthermore, if the mapping is nonlinear, composition with it may alter the numerator and denominator degrees of the rational approximating function and the zeros and poles of the latter will be moved. Therefore, the designer must accord due diligence when choosing the mapping.

2. *Mollify* $\tilde{H}_{even}(\tilde{\omega})$ *to a continuous and bounded variate function.* At points of discontinuity within $[-1, 1]$, the design requirements are modified in order to convert $\tilde{H}_{even}(\tilde{\omega})$ to $\tilde{H}_{cont}(\tilde{\omega})$, such that $\tilde{H}_{cont}(\tilde{\omega})$ is continous and of bounded variation. This mollification is an engineering design decision and depends on the particular problem to be solved. Generally, the modification is obtained by converting $\tilde{H}_{even}(\tilde{\omega})$ to a continuous function at its points of discontinuity.

3. *Compute Padé-Chebyshev rational approximation.* Because we will spectrally factor our Padé-Chebyshev approximation to achieve the desired network function $G_{ratl}(s)$, the function to be approximated is not $|\tilde{H}_{cont}(\tilde{\omega})|$ but $|\tilde{H}_{cont}(\tilde{\omega})|^2$. In order for $G_{ratl}(s)$ to attenuate for $s = j\omega$, $\omega \in [1, \infty)$, the degree of its numerator must be less than the degree of its denominator. However, as stated in Section 2.4, the Padé approximation $r_{m,n}(\omega)$ constructed by Geddes requires

$m > n$ [6]. Therefore, we reciprocate and, if necessary, truncate $|\tilde{H}_{cont}(\tilde{\omega})|^2$ to form $\max\left\{\frac{1}{|\tilde{H}_{cont}(\tilde{\omega})|^2}, A\right\}$ as the "target" for the rational approximation.

In our experience, the three conditions of Section 2.4 for successful execution of the Padé-Chebyshev construction have always been satisfied in network design applications. We suspect that increasing the numerator and denominator degrees of the approximant would overcome problems in this area if they arose. Choose m and n, with $m \geq n$, and calculate

$$c_k = \frac{2}{\pi}\int_{-1}^{1} \max\left\{\frac{1}{|\tilde{H}_{cont}(\tilde{\omega})|^2}, A\right\} \frac{T_k(\tilde{\omega})}{\sqrt{1-\tilde{\omega}^2}} d\tilde{\omega}.$$

Let $r_{m,n}(z)$ be the Padé approximation to $\sum_{k=0}^{m+n'} c_k z^k$, and compute the Padé-Chebyshev approximation,

$$\hat{R}_{m,n}(\tilde{\omega}) = \frac{r_{m,n}(\tilde{\omega} + j\sqrt{1-\tilde{\omega}^2}) + r_{m,n}(\tilde{\omega} - j\sqrt{1-\tilde{\omega}^2}}{2}.$$

4. *Define* $R_{m,n}(\tilde{s} = j\tilde{\omega}) = \frac{1}{\hat{R}_{m,n}(\tilde{s}/j)}$ *and analytically continue* $R_{m,n}(\tilde{s})$ *to the whole plane.*

5. *Spectrally factor the Padé-Chebyshev function.* For reasons we have discussed, $R_{m,n}(\tilde{s})$ will be even with real coefficients [11]. Thus it can be spectrally factored; retain the factor containing its left-half plane poles and zeros to form $\tilde{G}_{ratl}(\tilde{s})$.

6. *Return to the original domain by inverting the mapping in step 1 to yield* $G_{ratl}(s)$, which

    a. is rational, physically realizable

b. $|G_{ratl}(j\omega)| \simeq H_{spec}(\omega)$ on support of $H_{spec}(\omega)$, due to Padé-Chebyshev construction.

c. $|G_{ratl}(j\omega)| \to 0$ as $\omega \to \infty$ because denominator degree $>$ numerator degree.

7. *Iterate as necessary.* If the resultant magnitude frequency response does not satisfy the design specifications, the engineer may iterate this algorithm by 1) mollifying $H_{cont}(\omega)$, 2) adjusting m, n, or (m, n); while keeping $m > n$ in step 3, 3) adjusting the value of A, or 4) choosing a different mapping of the frequency axis.

Chapter 3

Examples

3.1 Double Bandpass Example

Problem: Determine a realizable transfer function implementing a double bandpass filter with center frequency of $\omega_0 = 0.75$ rad/sec, first pass band starting at $\omega = 0.4$, ending at $\omega = 0.5$; second pass band starting at $\omega = 1.0$, ending at $\omega = 1.3$; and notch attenuation ≤ -30 dB (gain≤ 0.0316), Figure 10.

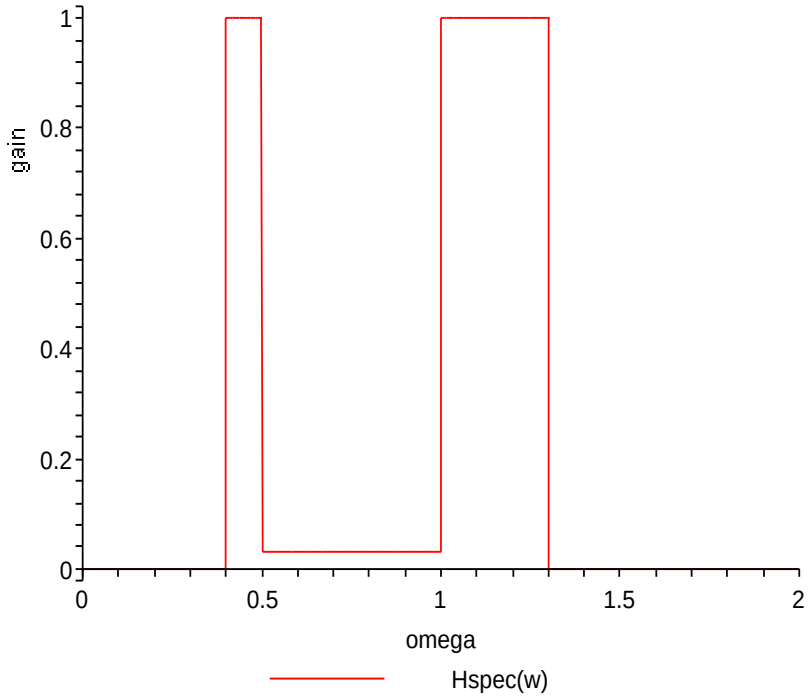

Figure 10. Design Requirements for Double Bandpass filter.

Step 1 uses a standard band pass mapping $\tilde{\omega} = 1.1111\omega - \frac{.5444}{\omega} : (0, \infty) \rightarrow (-\infty, \infty)$ [15] to define an even function $\tilde{H}_{even}(\tilde{\omega})$ with support on $[-1, 1]$, Figure 11. From Step 2 of our algorithm, we mollify $\tilde{H}_{even}(\omega)$, Figure 12. In order to compute the Padé-Chebyshev approximation, we form the reciprocal of $|\tilde{H}_{cont}(\tilde{\omega})|^2$ or $\frac{1}{|\tilde{H}_{cont}(\tilde{\omega})|^2}$ truncated at $A = (1/.0316)^2 = 1001$, Figure 13.

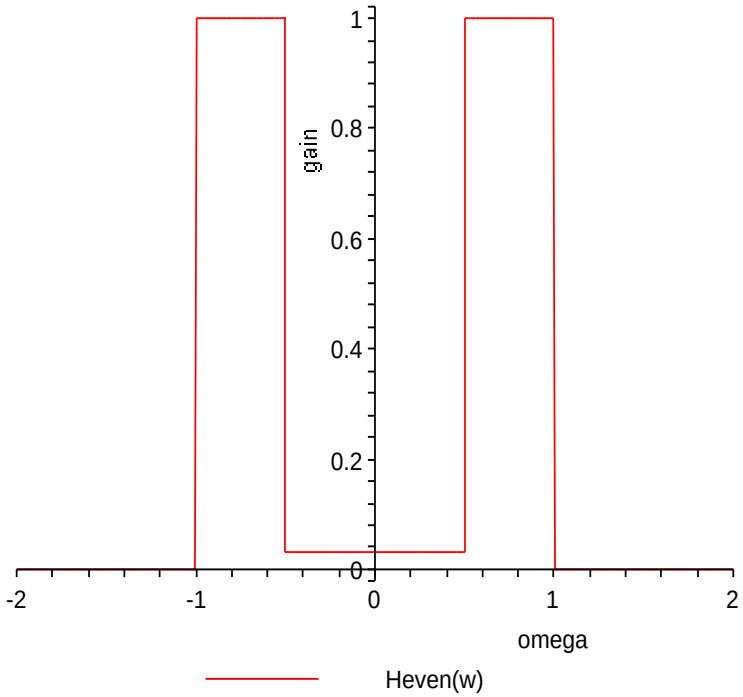

Figure 11. Even Function.

Equation 15 shows the result of applying Step 3 to Figure 13. In computing $r_{12,8}(\omega)$, we use the Chebpade command in Maple™. A comparison of the $\frac{1}{|\tilde{H}_{cont}(\tilde{\omega})|^2}$ versus the Padé-Chebyshev rational approximation, $r_{m,n}(\omega)$, is shown in Figure 14.

$$r_{12,8}(\tilde{\omega}) = \frac{\begin{array}{c} 32.858\,\tilde{\omega}^{12} - 152.94\,\tilde{\omega}^{10} + 288.19\,\tilde{\omega}^{8} \\ -274.50\,\tilde{\omega}^{6} + 140.74\,\tilde{\omega}^{4} - 36.430\,\tilde{\omega}^{2} + 3.7000 \end{array}}{2.1918\,\tilde{\omega}^{8} - 0.8989\,\tilde{\omega}^{6} + 0.3653\,\tilde{\omega}^{4} - 0.0472\,\tilde{\omega}^{2} + 0.0038} \tag{15}$$

For step 4, we substitute $\tilde{\omega} = \tilde{s}/j$ and reciprocate as depicted in equation (16).

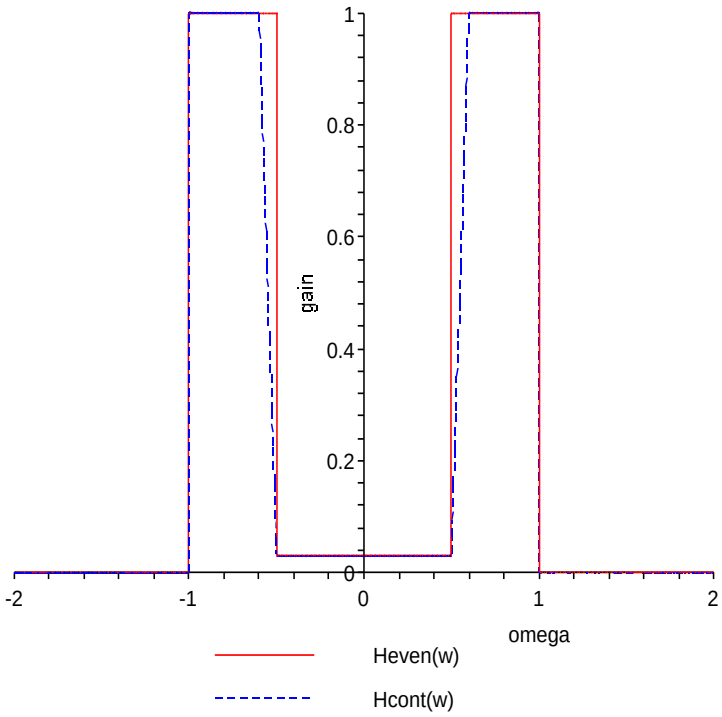

Figure 12. Mollified and Design Requirements.

$$R(\tilde{s}) = \frac{2.1918\,\tilde{s}^8 + 0.8989\,\tilde{s}^6 + 0.3653\,\tilde{s}^4 + 0.0472\,\tilde{s}^2 + 0.0038}{32.858\,\tilde{s}^{12} + 152.94\,\tilde{s}^{10} + 288.19\,\tilde{s}^8 + 274.50\,\tilde{s}^6 + 140.74\,\tilde{s}^4 + 36.430\,\tilde{s}^2 + 3.7000} \tag{16}$$

The spectral factor of $R(\tilde{s})$ with the appropriate zeros and poles from Step 5 is revealed in equation (17).

$$\tilde{G}_{ratl}(\tilde{s}) = 0.2569\,\frac{(\tilde{s}^2 + 0.6432\,\tilde{s} + 0.3327)\,(\tilde{s}^2 + 0.3082\,\tilde{s} + 0.1267)}{(\tilde{s}^2 + 0.4249\,\tilde{s} + 1.4897)\,(\tilde{s}^2 + 0.0251\,\tilde{s} + 0.3355)\,(\tilde{s}^2 + 0.3969\,\tilde{s} + 0.6713)} \tag{17}$$

Finally, $\tilde{G}_{ratl}(\tilde{s})$ is translated back to the original domain via the inverse band pass mapping [15], as revealed in equation (18) and simplified in equation (19).

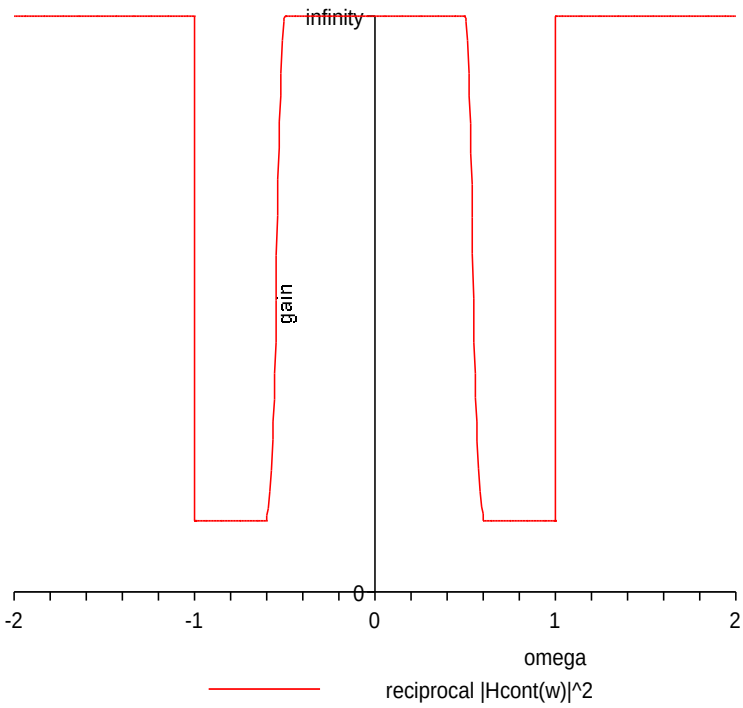

Figure 13. $max\left\{\frac{1}{|\tilde{H}_{cont}(\tilde{\omega})|^2}, A\right\}$ (Interpret "infinity" as A).

$$G_{ratl}(s) = \frac{\begin{array}{r} 0.2569\left(\left(1.1111\,s + \frac{0.5444}{s}\right)^2 + 0.7147\,s + \frac{0.3502}{s} + 0.3327\right) \\ \cdot\left(\left(1.1111\,s + \frac{0.5444}{s}\right)^2 + 0.3425\,s + \frac{0.1678}{s} + 0.1267\right) \end{array}}{\begin{array}{r} \left(\left(1.1111\,s + \frac{0.5444}{s}\right)^2 + 0.4721\,s + \frac{0.2313}{s} + 1.4897\right) \\ \cdot\left(\left(1.1111\,s + \frac{0.5444}{s}\right)^2 + 0.4410\,s + \frac{0.2161}{s} + 0.6713\right) \\ \cdot\left(\left(1.1111\,s + \frac{0.5444}{s}\right)^2 + 0.0278\,s + \frac{0.0136}{s} + 0.3355\right) \end{array}} \tag{18}$$

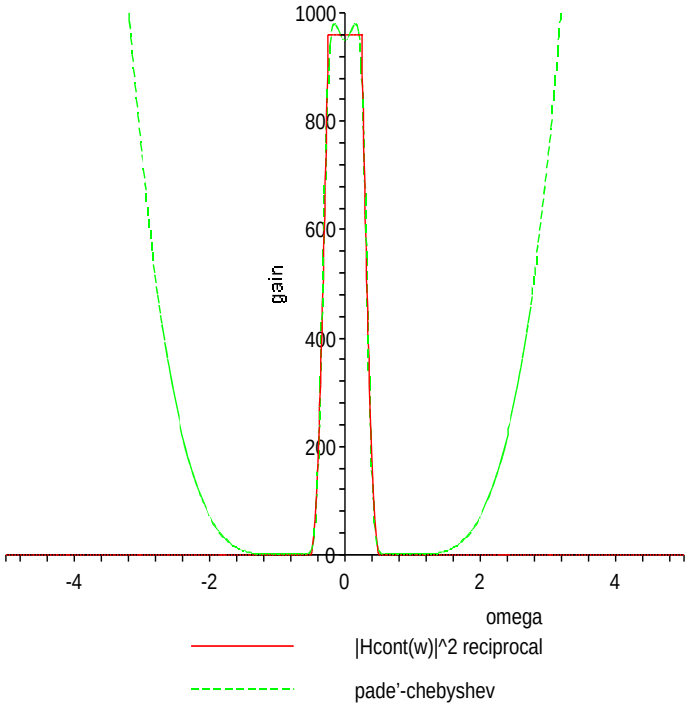

Figure 14. Design Goal vs. Approximation.

$$G_{ratl}(s) = \frac{\begin{array}{c} 0.3916\,s^{10} + 0.3353\,s^{9} + 0.9762\,s^{8} + 0.5444\,s^{7} \\ +0.7794\,s^{6} + 0.2673\,s^{5} + 0.2343\,s^{4} + 0.0394\,s^{3} + 0.0225\,s^{2} \end{array}}{\begin{array}{c} 1.8816\,s^{12} + 1.4343\,s^{11} + 9.6258\,s^{10} + 5.1749\,s^{9} + 17.0275\,s^{8} \\ +6.2399\,s^{7} + 12.8429\,s^{6} + 3.0575\,s^{5} + 4.0883\,s^{4} + 0.6088\,s^{3} + 0.5549\,s^{2} \\ +0.0405\,s + 0.0260 \end{array}} \tag{19}$$

Figures 15 and 16 compare Watanabe's result to our result (where a log-log axis are used to scale features). The main difference lies in the fact that all of Watanabe's poles and zeros lie solely on the $j\omega$ axis. This results in significant overshoot at the edges of transition of the passbands. In contrast, our result uses the Left-Hand side of the complex plane for its poles and zeros which results in smooth edge transitions.

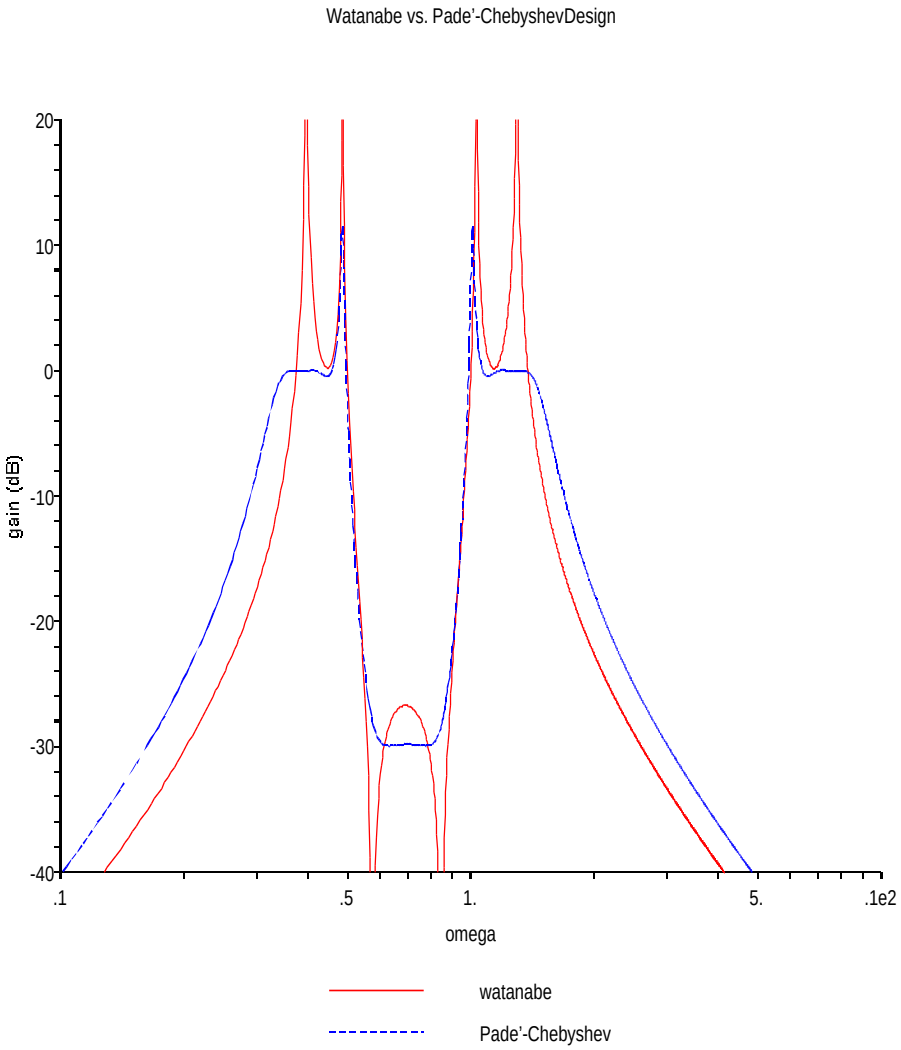

Figure 15. Watanabe vs. Padé-Chebyshev Frequency Response.

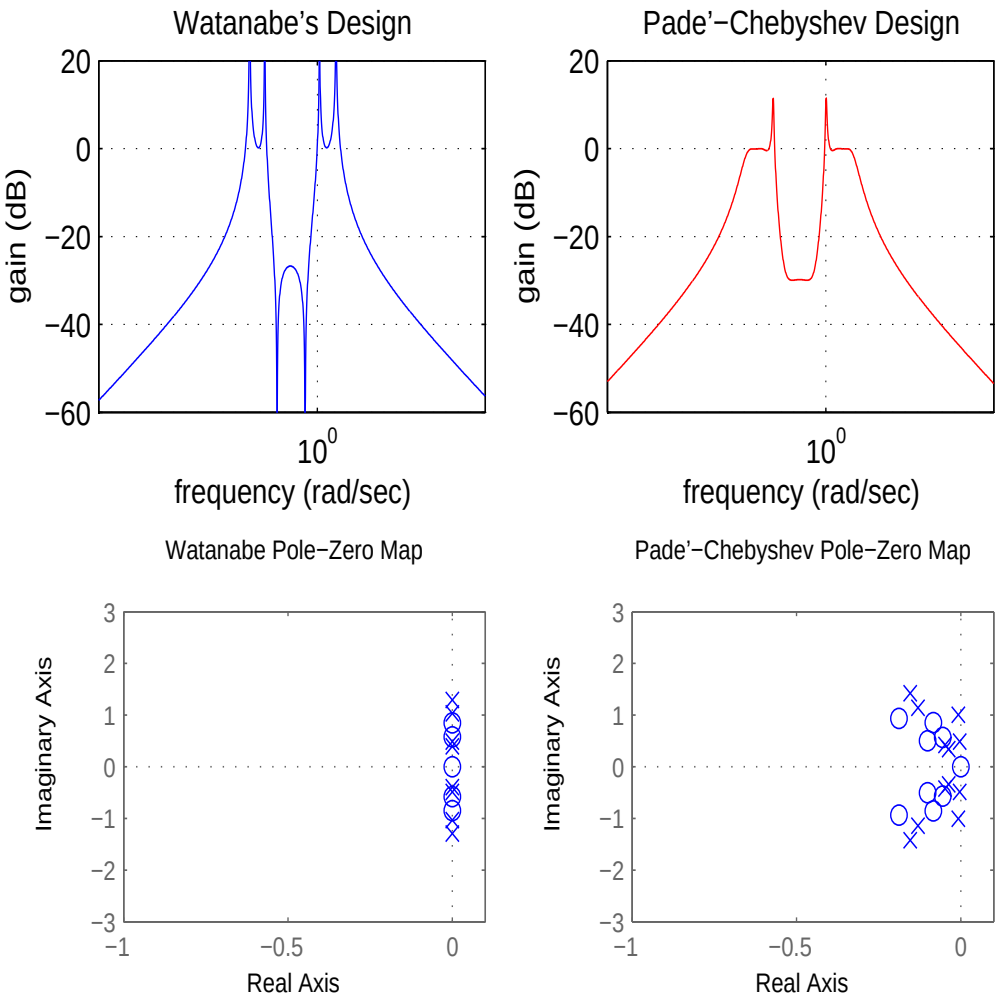

Figure 16. Watanabe vs. Padé-Chebyshev Frequency Response.

3.2 Ramp Example

Problem: Determine a realizable transfer function implementing a ramp filter. In Figure 17 is shown the ideal ramp function, often used in the process of impedance matching of transistor stages. For this example, the first two steps are not completely needed, since the specification is already continuous on its support and stated as a "lowpass". Instead, we need only extend $H_{spec}(\omega)$ to $\tilde{H}_{even}(\tilde{\omega})$, $\tilde{\omega} \in (-\infty, \infty)$ with support in [-1,1].

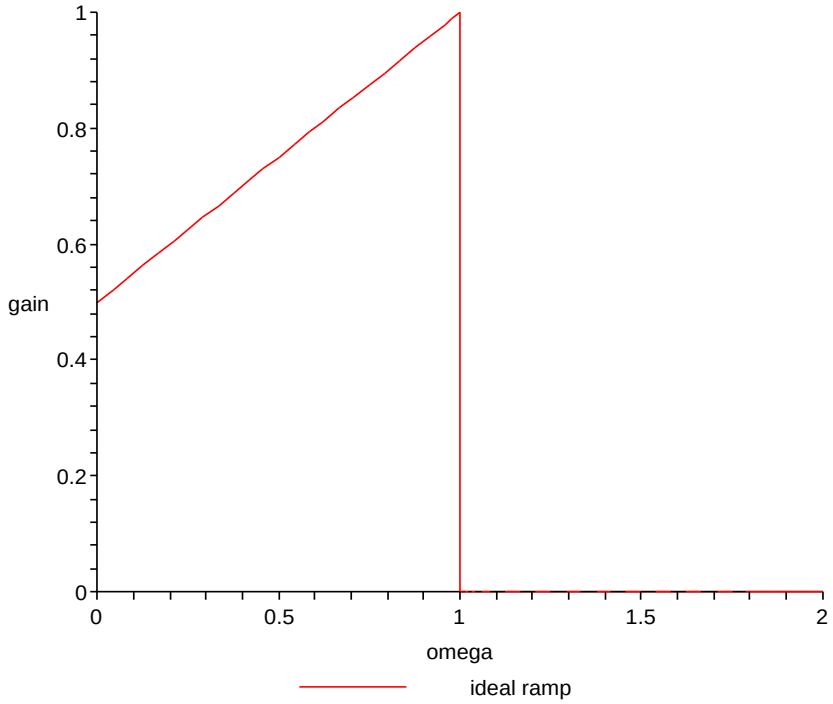

Figure 17. Ideal Ramp Frequency Response.

Before we compute the Padé-Chebyshev rational approximation $r_{m,n}(\tilde{\omega})$, the reciprocal is formed (A=10,000), Figure 18; with the result shown in equation (20). Figure 19 compares the $r_{10,4}(\tilde{\omega})$ with the reciprocal of $|\tilde{H}_{cont}(\tilde{\omega})|^2$.

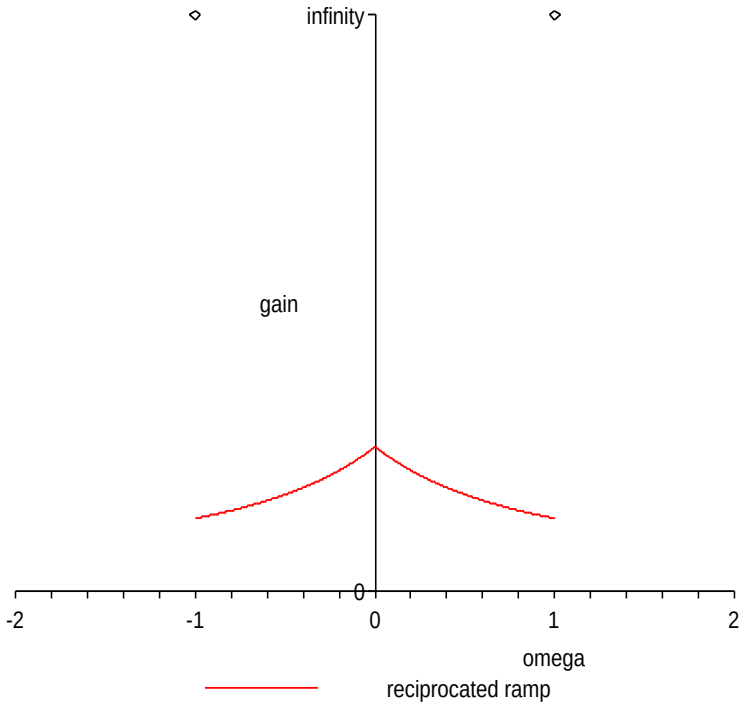

Figure 18. $max\left\{\frac{1}{|\tilde{H}_{cont}(\tilde{\omega})|^2}, A\right\}$ (Interpret "infinity" as A).

$$r_{10,4}(\tilde{\omega}) = \frac{\begin{array}{c}1.8826 - 2.0314\tilde{\omega}^2 + 1.6512\tilde{\omega}^4 \\ +0.4611\tilde{\omega}^6 - 0.0107\tilde{\omega}^8 + 0.0002\tilde{\omega}^{10}\end{array}}{1.0000 - 0.2835\tilde{\omega}^2 + 0.9891\tilde{\omega}^4} \tag{20}$$

Reciprocating and extending $r_{10,4}(\tilde{\omega})$ to the entire complex plane; i.e., replacing $\tilde{\omega}$ with $\tilde{s}/j$, results in equation (21).

$$R_{4,10}(\tilde{s}) = \frac{1.0000 + 0.2835\tilde{s}^2 + 0.9891\tilde{s}^4}{1.8826 + 2.0314\tilde{s}^2 + 1.6512\tilde{s}^4 - 0.4611\,\tilde{s}^6 - 0.0107\,\tilde{s}^8 - 0.0002\,\tilde{s}^{10}}. \tag{21}$$

Finally, the computed transfer function is revealed in equation (22) and shown in Figure 20 along with the ideal ramp.

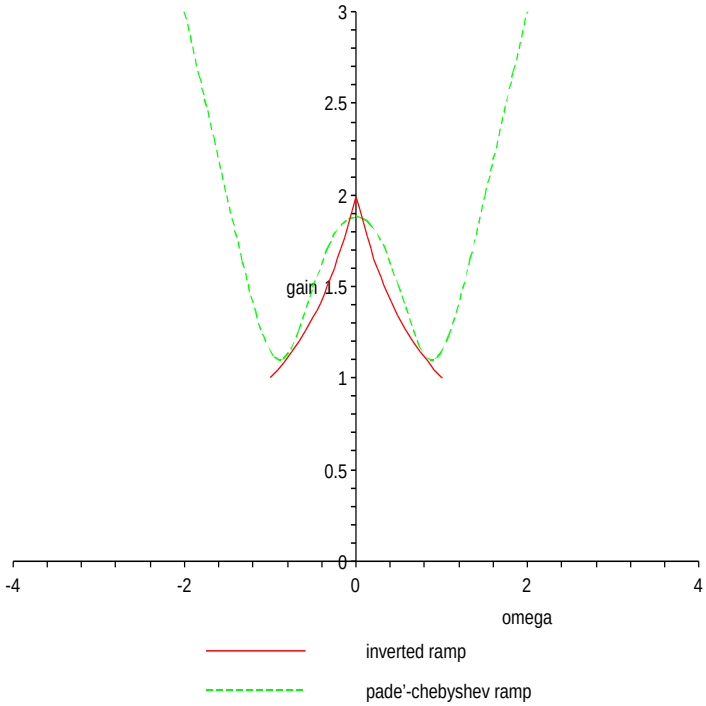

Figure 19. Reciprocal vs. Padé-Chebyshev Frequency Response.

The ramp transfer function was achieved with a relatively low order approximation. While this is good for implementation (especially for transistor circuits), if the given problem requires greater accuracy one could accomplish this by increasing either m, n, or (m,n).

$$G_{ratl}(s) = 79\,\frac{s^2 + 1.3131\,s + 1.0055}{(s + 2.0844)\,(s^2 + 6.4428\,s + 55.7993)\,(s^2 + 0.8637\,s + 0.9328)}. \quad (22)$$

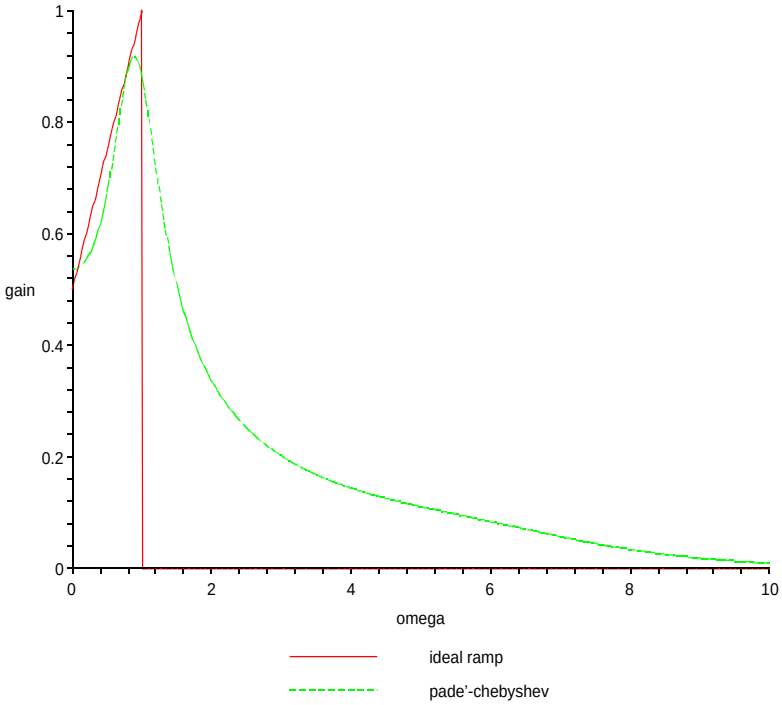

Figure 20. Ideal Ramp vs. Rational Transfer Function.

Chapter 4

Conclusion and Future Direction

4.1 Conclusion

Classical filter theory uses rational approximations that are reciprocals of polynomials, i.e., they have only poles and no zeros. (Note: Elliptic filters possess zeros and poles, but they restrict the placement of the zeros, i.e., the zeros are inversely related to the poles.) As a result, these approximants are too inflexible to approximate functions which have interior zeros, e.g., the double bandpass filter.

Herein, we have developed a new method that enables filter designers to approximate more general filter shapes by allowing arbitrary zeros and extending the use of the Padé algorithm. Previous attempts to match network transfer functions to general filter magnitude-frequency design requirements necessitated extremely complicated theory and formulation [16]. Watanabe's method (see summary in Appendix B) produces approximations that are sharper (due to imaginary axis poles and zeros); however, the author's method produces approximations that are smoother.

The author's algorithm is simpler in both concept and implementation. However, computing the Padé approximation in Step 3 is not without its numeric difficulties. High order Padé approximation sometimes requires the inversion of nearly singular matrices. In these situations, careful attention in choosing the matrix inversion algorithm is required.

The choice of the degrees of (m, n) and the mollification of $H_{spec}(\omega)$ are made so as to make the physical implementation of $G_{ratl}(s)$ as accurate as possible. However,

the lower the order of (m, n), the less the number of components required. Therefore, this conflict is resolved by an appropriate compromise (problem specific) for the selection of the degrees and mollification. The attenuation required of $|G_{ratl}(s = j\omega)|$ is achieved by increasing the denominator degree while keeping the numerator degree the same. The trade space among the design decisions then is (m, n), $H_{cont}(\omega)$, and attenuation. With experience, the engineer will reap successful designs for a broader class of problems previously unattainable with classical methods.

4.2 Future Direction

The algorithm presented herein is executed, in its present configuration, manually; i.e., the (m,n) and $\tilde{H}_{cont}(\tilde{\omega})$ are not software driven, rather user driven. An obvious extension is to automate our method so that the designer is not incumbered by these manipulations.

Another direction is to use this theory to compute phase-frequency specified rational functions. These types of functions (filters) are quite often used in communication systems to correct for timing errors (e.g., symbol errors).

Even though this paper has described a method of filter approximation, without modification it could be employed in another closely related field—Frequency Domain System Identification. Here the object is to find a realizable transfer function closely approximating a given set of measure data, $[F(\omega_k),\ \omega_k]$; where ω_k is a vector of discrete frequence points at which the system, $F(\omega)$, is measured.

References

[1] Norman Balabanian and Theodore Bickart. *Linear Netowrk Theory: Analysis, Properties, Design and Synthesis*. Matrix Series in Circuits and Systems. Matrix Publishers, Chesterland, Ohio, second edition, 1981.

[2] Richard L. Burden and J. Douglas Faires. *Numerical Analysis*, section 8.4, pages 517–529. Wadsworth Group, Pacific Grove, California, seventh edition, 2001.

[3] Richard L. Burden and J. Douglas Faires. *Numerical Analysis*, section 2.4, page 86. Wadsworth Group, Pacific Grove, California, seventh edition, 2001.

[4] Wai-Kai Chen. *Passive and Active Filters Theory and Implementations*, section 1.2, pages 10–119. John Wiley & Sons, Inc., New York, New York, second edition, 1986.

[5] J.C. Doyle, B. A. Francis, and A. Tannebaum. *Feedback Control Theory*, section 12.2, page 207. MacMillan Pub. Co., New York, New York, 1992.

[6] K. O. Geddes. Block structure in the chebyshev-padé table. *SIAM Journal on Numerical Analysis*, 18:844–861, 1981.

[7] T. N. T. Goodman, C. A. Micchelli, G. Rodriguez, and S. Seatzu. Spectral factorization of laurent polynomials. *preprint*, 1996.

[8] Lawrence P. Huelsman. *Active and Passive Analog Filter Design: An Introduction*, chapter 4, page 185. McGraw-Hill Series in Electrical and Computer Engineering. McGraw-Hill, Inc., New York, New York, 1993.

[9] George A. Baker Jr. and Peter Graves-Morris. *Padé Approximants*, volume 59 of *Encyclopedia of Mathematics and Its Applications*, section 7.4, page 386. Cambridge University Press, New York, New York, second edition, 1996.

[10] Shlomo Karni. *Applied Circuit Analysis*. John Wiley and Sons, New York, New York, 1988.

[11] R-C. Li. Always chebyshev interpolation in elementary function computations. *preprint*, 2002.

[12] J.C. Mason and D.C. Handscom. *Chebyshev Polynomials*, section 5.5, page 119. Chapman & Hall, Boca Raton, Florida, 2003.

[13] J.C. Mason and D.C. Handscom. *Chebyshev Polynomials*, section 5.5, page 125. Chapman & Hall, Boca Raton, Florida, 2003.

[14] H. Padé. Sur la répresentation appochée d'une fonction par des fractions rationelles. *Ann. Scientifique de l'Ecole Normale Supérieure*, 9:1–93, 1892.

[15] Kendall L. Su. *Analog Filters*, section 4.2, page 78. Chapman & Hall, London, UK, 1996.

[16] Hitoshi Watanabe. Approximation theory for filter-networks. *IRE Transactions on Circuit Theory*, pages 341–356, Sep 1961.

[17] L. Weinberg. *Network Analysis and Synthesis*, section 7.6, pages 331–333. McGraw-Hill, Inc., New York, New York, 1962.

Appendices

Appendix A: Symbol Glossary

Symbol	Meaning
ω	Frequency in rad/sec
$\tilde{\omega}$	Low pass prototype freqnuecy in rad/sec
s	Laplace domain variable
$\tilde{s}$	Low pass prototype domain variable
A	Reciprocal of maximum attenuation constant
$G_{ratl}(s)$	Desired network transfer function
$H_{spec}(\omega)$	Magnitude-squared design requirements
$\tilde{H}_{cont}(\tilde{\omega})$	Low pass prototype design requirements
$A(\tilde{\omega})$	Polynomial for LPP filters
$f(x)$	Generic function of x
$\tilde{f}(x)$	Taylor or Chebyshev series approximation of $f(x)$
$T_k(x)$	Chebyshev function of kth order
$\tilde{f}(z)$	Transformed $\tilde{f}(x)$ to unit circle
$r(x)$	Padé rational approximation to $\tilde{f}(x)$
$R(\tilde{s})$	Padé-Chebyshev rational approximation in LPP domain
$\tilde{G}_{ratl}(\tilde{s})$	Spectral factor of $R(\tilde{s})$

Appendix B: Watanabe's Double Bandpass Filter Theory

The attenuation and phase of the filter function are described as $w(\lambda) = u(\lambda) + jv(\lambda)$, where $w(\lambda)$ is the ideal transmission function, $u(\lambda)$ is the attenuation in nepers, and $v(\lambda)$ is the phase in radians. For the type of filters (attenuation only designs) presented in his work, only $u(\lambda)$ had special conditions that $w(\lambda)$ had to provide. These are

1. $u(\lambda)$ satisfies

$$u(\lambda) = A_k \text{ for } \lambda \in B_k$$

   where B_k's are given regions on the imaginary axis of the λ-plane, i.e., $B_k = [\pm b_{2k}, \pm b_{2k+1}]$, $k = 0, 1, 2, \ldots, n-1$.

2. The function

$$[u - \log|\lambda - a_i|]$$

   is regular at given points a_i, $i = 1, 2, \ldots, m$.

3. Otherwise, $u(\lambda)$ is a harmonic function.

A $w(\lambda)$ is called non-pole if it satisfies condition 1) and 3) only.

Theorem 1 *The ideal transmission function, $w(\lambda)$ is an Abelian integral of the third kind, and a non-pole $w(\lambda)$ is an Abelian integral of the first kind. They can be expressed as*

$$w(\lambda) = \int_\Gamma \psi \cdot d\lambda$$

see [16] for proof.

This means that the differential, $\psi \cdot d\lambda$, has the following properties:

1. $\psi \cdot d\lambda$ has poles of first order at the finite number of given points a_i's.

2. $\psi \cdot d\lambda$ has branch points of order 2 at the finite number of given points jb_{2k}'s and jb_{2k+1}'s.

Letting $S(p)$ denote the transmission function and $\phi(p)$ denote the characteristic function

$$G(p^2) = S(p)S(-p) = 1 + \psi(p^2) = 1 + \phi(p)\phi(-p).$$

Assume that the standard form of ideal transmission function, $w(\lambda)$, of a double bandpass filter has passbands $[-jk_1, +jk_1]$ and $[\pm j, \infty]$ and attenuation poles, Q_ν's, in the finite regions on the fundamental plane. From the general theory in Section III in [16], the ideal transmission function is given as

$$w(\lambda) = \int_0^\lambda \left\{ d_\infty + \sum_{\nu=1}^{m} \frac{d_\nu}{\lambda^2 + Q_\nu^2} \right\} \frac{d\lambda}{\sqrt{(\lambda^2 + k_1^2)(\lambda^2 + 1)}} \tag{23}$$

where $\lambda_i = d_i + jQ_i$. This integral is an elliptic integral of the third kind. It is known that the characteristic function, $\phi(p)$, of a double bandpass filter can be found without solving any transcendental equations if and only if the integral (23) is expressed in the form of

$$w(\lambda) = \sum_{\mu=1}^{N} \gamma_\mu w_\mu(\lambda)$$

$$w_\mu(\lambda) = \alpha \sinh^{-1} X_\mu(\lambda)$$

where $X_\mu(\lambda)$ is an algebraic function of λ and α is a constant. $w_\mu(\lambda)$ is defined as the canonical form of $w(\lambda)$ for a double bandpass filter.

Appendix B (Continued)

Theorem 2 *The necessary and sufficient conditions for an ideal transmission function, $w(\lambda)$, for a double bandpass filter to be in canonical form are:*

1. *All residues of differential, $dw(\lambda)$ are ± 1.*
2. *There exist polynomials $A(\lambda)$, $B(\lambda)$, and $R(\lambda)$ that satisfy*

$$(\lambda^2 + k_1^2)(\lambda^2 + 1)R^2(\lambda) = A(\lambda)B(\lambda), \tag{24}$$

$$\prod_{\nu=1}^{m}(\lambda^2 + Q_\nu^2) = A(\lambda) - B(\lambda). \tag{25}$$

See [16] for proof.

Corollary 3 *The canonical form of $w(\lambda)$ for a double bandpass filter can be written*

$$w_\mu(\lambda) = 2\sinh^{-1}\sqrt{\frac{-A(\lambda)}{\prod_{\nu=1}^{m}(\lambda^2 + Q_\nu^2)}}.$$

From Theorem 6, it is known that one polynomial of $A(\lambda)$ or $B(\lambda)$ is of order $2m$ and the other is of order, at most, $(2m-2)$. Hence, from (24), $R(\lambda)$ must be an odd polynomial of order, at most, $(2m-3)$, and is expressed as

$$R(\lambda) = R \cdot \lambda \prod_{i=1}^{m-2}(\lambda^2 + \alpha_i^2) \tag{26}$$

where R and α_i are $(m-1)$ unknown parameters. By (24), (25), and (26); we get m relations for the parameters R, α_i, Q_ν, and k_1.

$$F_k(R, \alpha_i, Q_\nu, k_1) = 0, \ k = 1, 2, \ldots, m. \tag{27}$$

Appendix B (Continued)

For (27) to be valid, it is necessary for one condition to be satisfied

$$F(Q_\nu, k_1) = 0, \tag{28}$$

which is obtained by eliminating $(m-1)$ R and α_i unknown parameters. Condition (28) is defined as the characteristic condition for the double bandpass filter. Thus *any double bandpass filter with attenuation poles, Q_ν, and band ratio, k_1, becomes possible of realization without solving any transcendental equations, provided that the characteristic condition (28) is established.*

By taking a linear combination of various canonical ideal transmission functions having the same band factor, k_1, and various attenuation poles, Q_ν, which satisfy (28), the general ideal transmission function can be written

$$w(\lambda) = \sum_{\mu=1}^{N} \gamma_\mu \cdot \left\{ 2 \sinh^{-1} \sqrt{\frac{-A_\mu(\lambda)}{\prod_{\nu=1}^{m}(\lambda^2 + Q_\nu^2)}} \right\} \tag{29}$$

Equation (29) can be transformed, see Theorem 2 in [16], by

$$\phi(\lambda) = H \cosh w(\lambda)$$

into

$$\phi(\lambda) = H \frac{\mathcal{RA}[\prod_{\mu=1}^{N} \{\sqrt{A_\mu(\lambda)} + \sqrt{B_\mu(\lambda)}\}^{2\gamma_\mu}]}{\prod_{\mu=1}^{N} \prod_{\nu=1}^{m} (\lambda^2 + Q_{\mu\nu}^2)^{\gamma_\mu}}, \tag{30}$$

where $\mathcal{RA}$ means rational part of the function. According to Theorem 2, (30) will exhibit Tschebysheff performance in the pass band, but not in the stop band.

Appendix C: Filter Transformations

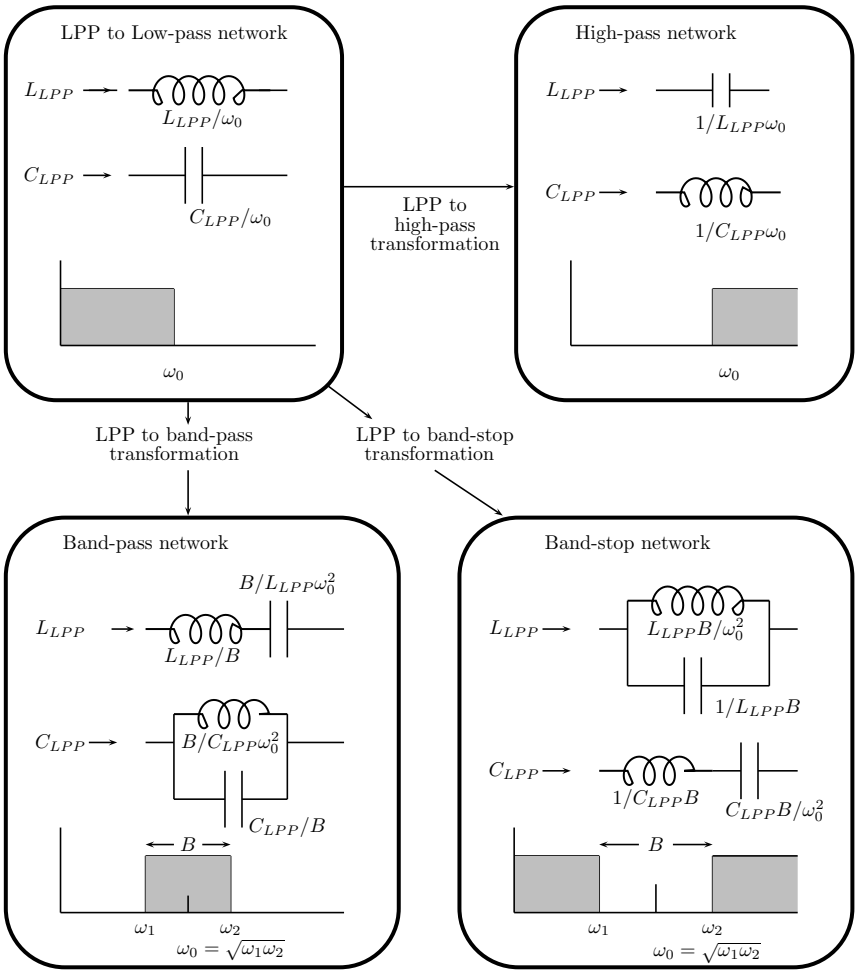

Figure 21. Filter Transformations.

About the Author

William Joel Dietmar Johnson is a well balanced individual with plenty of experience in everything. He is an expert marksman as well as an expert RF designer. He can pack dishwashers optimally as well as car trunks and moving boxes. He tends to accumulate expensive things like books, motorcycles, and firearms. He also speaks foreign languages and has lived and traveled extensively throughout the world, including Asia.